

## Specification of cell fates at the dorsal margin of the zebrafish gastrula

Anna E. Melby<sup>1,\*</sup>, Rachel M. Warga<sup>2,†</sup> and Charles B. Kimmel<sup>1</sup>

<sup>1</sup>Institute of Neuroscience, University of Oregon, Eugene, Oregon, 97405, USA

<sup>2</sup>Max-Planck-Institut für Entwicklungsbiologie, Spemannstrasse 35/III, 72076 Tübingen, Germany

\*Present address: Department of Biochemistry, Box 357350, University of Washington, Seattle, WA 98195-7350, USA

†Present address: Institute of Neuroscience, University of Oregon, Eugene, Oregon, 97405, USA

### SUMMARY

Using fate mapping techniques, we have analyzed development of cells of the dorsal marginal region in wild-type and mutant zebrafish. We define a domain in the early gastrula that is located just at the margin and centered on the dorsal midline, in which most cells generate clones that develop exclusively as notochord. The borders of the notochord domain are sharp at the level of single cells, and coincide almost exactly with the border of the expression domain of the homeobox gene *floating head* (*flh*; zebrafish homologue of *Xnot*), a gene essential for notochord development. In *flh* mutants, cells in the notochord domain generate clones of muscle cells. In contrast, notochord domain cells form mesenchyme in embryos mutant for *no tail* (*ntl*; zebrafish homologue of *Brachyury*).

A minority of cells in the notochord domain in wild-type embryos develop as unrestricted mesoderm, invariably located in the tail, suggesting that early gastrula expression of *flh* does not restrict cellular potential to the notochord

fate. The unrestricted tail mesodermal fate is also expressed by the forerunner cells, a cluster of cells located outside the blastoderm, adjacent to the notochord domain. We show that cells can leave the dorsal blastoderm to join the forerunners, suggesting that relocation between fate map domains might respecify notochord domain cells to the tail mesodermal fate. An intermediate fate of the forerunners is to form the epithelial lining of Kupffer's vesicle, a transient structure of the teleost tailbud. The forerunners appear to generate the entire structure of Kupffer's vesicle, which also develops in most *flh* mutants. Although forerunner cells are present in *ntl* mutants, Kupffer's vesicle never appears, which is correlated with the later severe disruption of tail development.

Key words: fate map, notochord, axis, organizer, tail, *floating head*, *Xnot*, *no tail*, *Brachyury*, zebrafish

### INTRODUCTION

During development, cells undergo changes in behavior and gene expression that distinguish them from their neighbors. We refer to these changes as specification, a conditional process that may bias the development of a cell, but not necessarily restrict its developmental potential (Davidson, 1990, 1993; Kimmel et al., 1991). We seek to understand how cell fates are specified by fate mapping the normal locations of early progenitor cells that give rise to specific tissues (Slack, 1991), observing how these fate map domains correspond to the domains of expression of developmental regulatory genes, and observing how fate maps are changed by mutations in these genes.

A region of considerable interest in the vertebrate embryo is that which develops axial mesoderm, in particular the notochord. In the zebrafish, *Danio rerio*, this region is located at the dorsal margin of the blastoderm (Kimmel et al., 1990), and in the early gastrula it can be recognized as a local cellular condensation along the marginal germ ring, termed the embryonic shield. The embryonic shield of the teleost embryo corresponds approximately to the Spemann organizer (Oppenheimer, 1936; Ho, 1992), the dorsal lip region of the amphibian

gastrula that is capable of inducing a second body axis when transplanted to the ventral side of another embryo (Spemann and Mangold, 1924). The notochord is derived from cells within the embryonic shield, and plays a key role in patterning the body axis and establishing dorsoventral polarity in adjacent tissues (Yamada et al., 1991; Koseki et al., 1993; Halpern et al., 1993; Fan and Tessier-Lavigne, 1994).

Mutations in two genes that affect notochord development have been described in zebrafish: *floating head* (*flh*), a homeobox gene homologous to the *Xenopus* gene *Xnot* (Talbot et al., 1995; von Dassow et al., 1993; Gont et al., 1993), and *no tail* (*ntl*), the zebrafish homologue of the mouse gene *Brachyury* (Schulte-Merker et al., 1994b), which encodes a transcription factor (Kispert and Herrmann, 1993). No notochord develops in zebrafish embryos homozygous for mutations in either of these genes. Both mutants have characteristic, distinctive changes in the midline location that the notochord would occupy in wild types. In *flh* mutants, the somites fuse in the midline underneath the neural tube, and midline mesodermal cells express markers characteristic of paraxial mesoderm (Halpern et al., 1995). By the pharyngula period, when cells have begun to differentiate, muscle develops in the midline (Talbot et al., 1995). In contrast, somites do not

fuse across the midline in *ntl* mutants; instead mesenchymal cells occupy the midline position. These cells have been interpreted to be blocked notochord precursors (Halpern et al., 1993), and they express markers characteristic of developing notochord (Krauss et al., 1993).

A variety of cell fates arise from the embryonic shield (Kimmel et al., 1990), but precisely how these fates are arranged in wild-type embryos, and how cell fate domains are changed in *flh* and *ntl* mutants are not understood. To address these issues, in the present study we have constructed a detailed fate map for a subset of cells in this region by single cell labeling with lineage tracer dye. We show that most, but not all, cells in the shield region that we mapped give rise to tissue-restricted clones. We identify a notochord fate map domain at the midline, and show that it coincides with the expression domain at the same stage of the *flh* gene. Cells of the notochord domain develop as muscle in *flh* mutants, suggesting that the wild-type *flh* gene plays a key role in causing cells to adopt a notochord rather than a muscle fate. Cells of the notochord domain form mesenchyme in *ntl* mutants, confirming previous results (Halpern et al., 1993).

Our fate map studies also reveal that a minority of cells near the margin in the embryonic shield, irrespective of their fate map domains, generate unrestricted clones of mesoderm located in the caudal-most part of the tail. These cells possibly become respecified to these caudal fates by relocating from the blastoderm to join the forerunner cell domain, located adjacent to the dorsal blastoderm margin. We have characterized the development of forerunner cells, and discovered that in wild-type embryos they transiently form the epithelial lining of a structure known as Kupffer's vesicle, an enigmatic teleost speciality present in the tailbud (reviewed by Nordahl, 1970). Kupffer's vesicle develops in most *flh* mutants, but not at all in *ntl* mutants, correlating with the severe tail deficiency in *ntl* mutant embryos, and suggesting that formation of the vesicle may be required for tail development.

## MATERIALS AND METHODS

### Fish stocks

Gastrula fate mapping was performed on wild-type embryos, and embryos homozygous for *golden* (*gol<sup>b1</sup>*), a mutation affecting melanin production (Streisinger et al., 1986). Analysis of cell fate in *flh* and *ntl* mutants was performed on embryos derived from matings of *flh<sup>n1</sup>* heterozygotes, and *ntl<sup>b160</sup>* or *ntl<sup>b195</sup>* heterozygotes, respectively. *flh<sup>n1</sup>* (Talbot et al., 1995), *ntl<sup>b160</sup>*, and *ntl<sup>b195</sup>* (Schulte-Merker et al., 1994b) are all putative null alleles. Wild-type and mutant embryos were indistinguishable at the time of labeling; genotypes were determined during the early pharyngula period (24–36 hours postfertilization at 28.5°C, Kimmel et al., 1995), when cell fates were determined. Phenotypically wild-type embryos served as controls for the mutants and were also used for the wild-type fate map.

To learn whether dorsal marginal cells can enter the forerunner cell population, early blastomere labeling was performed with wild-type embryos or with *gol<sup>b1</sup>* or *sparse* (*spa<sup>b134</sup>*) homozygous mutants. *spa* causes a reduction of melanophores; *gol* and *spa* were therefore used because their 2 day to 4 day (d) embryos have greater optical clarity than wild-type embryos.

### Cell labeling and fate determination

Embryos were maintained at 28.5°C, except during labeling, which was done at room temperature (about 22°C). Cells were injected at the shield stage of the early gastrula (Kimmel et al., 1995), 5.5–6 hours after fertilization (h). At shield stage, involution has begun and the embryonic

shield is visible on the dorsal side of the embryo (Fig. 1). Cells were injected with 1–2% rhodamine dextran ( $10 \times 10^3 M_r$ , Molecular Probes) as described by Raible et al. (1992). To allow for easy repositioning, embryos were mounted dorsal side up in 3–4% methyl cellulose covered with embryo medium (Westerfield, 1993). We labeled only the most superficial layer of deep cells in the epiblast, those positioned just below the enveloping layer (EVL). Deep cells give rise to the embryo while EVL cells form the extra-embryonic periderm (Kimmel et al., 1990). Labeling was done using a long working distance 40× water-immersion objective on an upright Zeiss Standard microscope, equipped with Nomarski and fluorescence optics. The dye-filled electrode was lowered until it could just be seen to dimple the surface of the cell, and then the cell was simultaneously penetrated and filled with dye by oscillating negative capacitance through the electrode. The effectiveness of the labeling was monitored visually. When two cells were labeled and later gave rise to multiple fates, the data were uninterpretable for the fate map. Data from pairs of labeled cells were used for the fate map only if the progeny of both cells were confined to a single tissue. EVL cells were often also labeled, but did not complicate the analysis since they have a distinct morphology and do not contribute to embryonic tissues.

The location of a cell in the fate map was determined by measuring two coordinates: its distance from the margin and its distance from the dorsal midline. The distance from the margin was determined by counting cell diameters immediately after labeling. Next, fluorescent and bright-field images of the embryo in both dorsal and animal pole views (Fig. 1A,B) were collected using a Macintosh Ilci running AxoVideo software (Myers and Bastiani, 1991; Axon Instruments), which operated a Pulnix camera coupled to a video intensifier (Dark Invader). Images were recorded using an optical disc recorder (Panasonic). The distance from the dorsal midline was determined by measuring the angle between the midline and the labeled cell from the video image of the animal pole view. The angle was converted to cell diameters to simplify the graphs (Figs. 3 and 4), setting one cell diameter to equal 3° of arc. Embryos were labeled individually, and cells were localized immediately after labeling.

Cells fates were determined by examining the position and morphology of labeled cells in live embryos during the early pharyngula period, and often again at 2d and 3d. Images were obtained using a silicon intensified camera (Dage-MTI, Inc.) mounted on an intensifier tube (Videoscope) on a Zeiss Universal microscope. The camera was connected to a Macintosh Quadra running AxoVideo, and images were recorded with an optical disc recorder. Adobe Photoshop 3.0 was used to add pseudocolor and to merge fluorescent and bright-field images taken at the same focal plane.

Caged fluorescein dextran ( $10 \times 10^3 M_r$ , Molecular Probes) was used as a lineage tracer to follow the development of the population of forerunner cells. Embryos were filled with caged fluorescein dextran by injecting dye into the yolk cell at the 2–8 cell stage (Ho and Kane, 1990), kept in the dark and viewed only with tungsten-based light, to prevent uncaging of the dye. Forerunner cells were labeled by uncaging the dye in the early gastrula period (shield stage to 60% epiboly) using a DAPI filter setting on a Leitz Laborlux S microscope. Embryos were mounted dorsal side up in methyl cellulose on a depression slide. The diaphragm between the fluorescent light source and the embryo was closed down such that at a magnification of 400×, only 3–4 cells were illuminated. The embryo was held in one place under this spot of illumination for a few seconds and gradually relocated by moving the stage, until the entire forerunner cell population had been exposed. The success of labeling was checked visually, then the embryo was left to develop in the dark. Later the embryo was observed using the Zeiss Universal microscope and image-processing set-up described above. Embryos labeled with caged fluorescein were viewed infrequently since it appeared that the fluorescence emitted from labeled cells was capable of uncaging dye in adjacent cells.

In experiments to examine whether dorsal marginal cells can join the forerunner cell population, single marginal blastomeres were labeled at midblastula stages (from the 1000-cell stage to high stage)

by pressure injecting a mixture of 2% rhodamine dextran ( $10 \times 10^3 M_r$ , Molecular Probes) mixed with 1% lysinated biotin dextran ( $10 \times 10^3 M_r$ , Molecular Probes; see Kimmel and Warga, 1987). Labeling was done at a magnification of 125 $\times$  or 200 $\times$  on a Zeiss Universal microscope adapted with stage-mounted micromanipulators. Embryos were checked immediately after labeling and those with labeled cells coupled to the yolk cell were discarded. From 40% epiboly through the late shield stage, embryos were mounted dorsal side up in 3–4% methyl cellulose and the location of labeled cells with respect to the margin and the forerunner cell population was determined. Cell fate was determined in vivo from 1d–4d; embryos were subsequently fixed and processed for whole-mount staining of biotin dextran (Westerfield, 1994). Fluorescent images of embryos were obtained using a Newvicon camera (Videoscope International, L.T.D.) mounted on an intensifier tube (Videoscope International, L.T.D.) on a Zeiss Axioscope, and recorded directly onto an optical disc recorder (Sony).

### Histological methods

RNA in situ hybridizations were performed essentially as described by Thisse et al. (1993), eliminating alkaline hydrolysis of probes, treatment with proteinase K, and the dehydration-rehydration steps prior to hybridization. Embryos were hybridized at 65°C. Double RNA in situ hybridization with *flh* and *gooseoid* (*gsc*) probes was performed on whole mounts, as described by Jowett and Lettice, (1994); Hauptmann and Gerster (1994). Following staining, embryos were embedded in agar and frozen sections were cut.

For mapping of the *flh* expression domain, cells in shield stage embryos were labeled with fixable lysinated fluorescein dextran ( $3,300 M_r$  or  $10 \times 10^3 M_r$ , Molecular Probes). The position of the labeled cell was determined in the live embryo, then the embryo was fixed immediately in 4% paraformaldehyde buffered in PBS, stored in fixative at 4°C for 1–2 days, and processed for immunohistochemistry (to detect the lineage tracer) using a peroxidase-conjugated anti-fluorescein antibody (Boehringer-Mannheim). Following immunohistochemistry, embryos were processed for in situ hybridization with anti-sense *flh* RNA (Talbot et al., 1995). At the early gastrula stage, *flh* is expressed strongly in the dorsal marginal region, but also shows weaker expression in lateral bands that are a slight distance from the margin, and in the forerunner cells (Melby et al., unpublished data). The color reaction was only allowed to proceed for 1 hour so that the staining was confined to the central, strongly expressing region. Embryos were cleared in glycerol and examined at 160 $\times$  magnification to estimate the border of *flh* staining relative to the labeled cell.

Embryos processed for RNA in situ hybridization with *ntl* probe were dehydrated in methanol, cleared with methyl salicylate, and mounted on bridged slides in Permount (Melby et al., unpublished data). Embryos stained for biotin were dehydrated in ethanols and mounted between bridged coverslips in Permount (Westerfield, 1994).

## RESULTS

### A coherent notochord fate map domain is present at the dorsal margin of the early gastrula

Understanding the character of fate map domains is a prerequisite for meaningful analysis of the mechanisms that underlie development of specific tissues. We have used lineage-tracer dye injections into single cells in the early gastrula (shield stage, 6h, Fig. 1) to precisely locate notochord precursors, that we later identify by examining their descendent clones of labeled cells in the pharyngula (Fig. 2). We found that notochord-forming cells are centered on the dorsal midline near the blastoderm margin, in an area well-known in teleost embryos as the embryonic shield. We thoroughly explored the

fates of the outer layer of epiblast cells in the embryonic shield, as well as a distinctive population of cells separate from the blastoderm (forerunner cells, see below) to obtain the fate maps shown in Figs 3 and 4.

The notochord is the predominant fate of the cells we examined in the embryonic shield (Table 1). Moreover, notochord progenitors nearly all fall within a clear, well-circumscribed region centered on the dorsal midline (2 exceptions in Fig. 4A). The notochord fate map domain extends about 7 cell diameters to either side of the midline, and about 4 cell diameters away from the blastoderm margin towards the animal pole (outline drawn on graphs in Figs 3 and 4). Most of the notochord-forming clones deriving from this circumscribed region are tissue-restricted, i.e. the clonally related progeny are restricted to a single tissue or organ type, in this case, the notochord (open circles; Figs 3A and 4A). Tissue-restriction tends to be the rule for those cells whose progeny come to be located in the trunk or head of the pharyngula (data collected in Fig. 3A–E). We treat the tail separately below.

Among the labeled cells in such notochord-restricted clones we observe two morphologically distinguishable cell types that comprise the notochord organ: large vacuolated structural cells (Fig. 2C), and thin squamous epithelial cells of the notochord sheath (Fig. 2D). Both cells types are often present in single clones arising from one early gastrula progenitor (see Fig. 2A–D). The developing notochord forms, after gastrulation, as a stack of coin-shaped cells along the midline. Both definitive notochord cell types later derive from these coin-shaped cells (data not shown).

Cells just outside the notochord domain that contribute to other fates in the trunk and head are also mostly tissue-restricted. On either side of the notochord fate map domain near the blastoderm margin are cells fated to form trunk body wall muscle (Fig. 3B). Cells contributing to head mesenchyme and to the hatching gland (that derives from the prechordal plate; Kimmel et al., 1990; Fig. 3C and D), are located just at, or immediately adjacent to, the margin.

Superficial epiblast cells near the dorsal midline but farther from the margin (beginning about four cell diameters away from the margin) generate clones restricted to the central nervous system (Fig. 3E). These clones were usually located in the ventral spinal cord. However, as for the example in Fig. 2I, they almost always excluded the floor plate, which is a single midline row of cells in zebrafish (Hatta et al., 1991). We observed only two cases in which an outermost epiblast cell gave rise to floor plate: one contained a string of floor plate in the tail; the other contained floor plate, adjacent neural cells, and fin mesenchyme in the tail. In order to locate floor plate precursors, we explored the fates of cells lying at deeper levels in the embryonic shield, and observed that cells one or two diameters deep to the region of neural precursors shown in Fig. 3E generated floor plate ( $n=8$ ; Fig. 2J).

Cells that contribute to the notochord in the pharyngula tail (Fig. 4A) evidently are more scattered than those that contribute to the trunk notochord (Fig. 3A). Forerunner cells, as well as blastoderm cells, contribute to tail notochord, and tail notochord-forming cells frequently are not lineage-restricted to the notochord (closed circles, Fig. 4A). Within the notochord domain there exists a significant minority of cells that are unrestricted tail mesoderm precursors, contributing not only to notochord, but also to tail muscle (Fig. 4B), and tail mes-

**Table 1. Summary of fate map data**

Tissue precursor	Total number of cells in fate map*	Number of single cells labeled	Clone size mean $\pm$ s.d.
Trunk notochord†	60	44	4.07 $\pm$ 1.54
Tail notochord†	20	10	3.30 $\pm$ 1.34
Trunk muscle†	15	13	2.69 $\pm$ 1.03
Tail muscle†	4	4	5.40 $\pm$ 1.34
Head mesenchyme	9	7	12.71 $\pm$ 5.99
Nervous system†	17	11	9.91 $\pm$ 4.55
Hatching gland†	2	2	n.d.
Tail mesoderm:			
blastoderm	11	11	6.90 $\pm$ 1.97
forerunner cells‡	11	6	7.00 $\pm$ 3.22

\*Includes single cells and pairs of labeled cells that contributed to the same fate.  
†Numbers are for tissue-restricted precursors only.  
‡Includes both tissue-restricted and unrestricted forerunner cells.

enchyme (Fig. 4D,E). The clones produced by these cells resemble those produced by the forerunner cells (see below).

### The expression domain of *flh* corresponds to the notochord fate map domain in the early gastrula

Finding that cells contributing to the trunk notochord lie within a well-defined fate map domain might mean that the cells within the domain have been specified, through the action of developmental regulatory genes, to develop the notochord fate. A candidate gene for such specification is *flh*, since this gene is required for notochord development and since, in the early gastrula, *flh* is expressed specifically in the embryonic shield (Talbot et al., 1995). Based on this possibility, we used two kinds of double-labeling procedures to examine more closely the *flh* expression domain in the early gastrula relative to the notochord fate map domain.

Fixation and in situ hybridization cause tissue shrinkage and a loss of cellular resolution in stained embryos. Therefore, to precisely compare the borders of *flh* expression and the notochord fate map domain, we first injected lineage tracer dye into one cell that we judged to be on or near the notochord fate map domain borders in the superficial epiblast, in a series of live embryos. We determined these cells' position within the fate map, then immediately fixed and processed these embryos to show simultaneously both the marked cell and the region of *flh* expression (Fig. 5A). We determined the border of the region of strong *flh* expression relative to the marked cell and found that it was always exactly on or adjacent to the border of the notochord fate map domain (Fig. 5B). The variability we observed, on the order of 1-2 cell diameters, is comparable to that in establishing the fate map domain borders themselves, and we probably can attribute it to experimental error in correctly locating a fate map domain border in the live gastrula.

Another putative developmental

**Table 2. Presence or absence of Kupffer's vesicle between the 5-somite and 10-somite stage**

Embryo class	Number	Number with Kupffer's vesicle	% with Kupffer's vesicle
<i>ntl</i> mutants	75	0	0
Wild-type sibs of <i>ntl</i> mutants	209	204	97.61
<i>flh</i> mutants	136	102	75
Wild-type sibs of <i>flh</i> mutants	383	370	96.61

Embryos were scored using a Wild stereomicroscope at 50 $\times$  magnification.

regulatory gene, *gooseoid* (*gsc*), is expressed in the early gastrula dorsal marginal zone, apparently in cells that will go on to form prechordal plate (Stachel et al., 1993; Schulte-Merker et al., 1994a; Thisse et al., 1994), a principal derivative of which is the hatching gland (Warga, 1996), but not the notochord. At the early gastrula stage we fate mapped, most *gsc*-expressing cells have already involuted into the hypoblast (see particularly Thisse et al., 1994). However, *flh*-expressing cells are confined to the epiblast, the region we determined gives rise to notochord (Talbot et al., 1995). Double-labeling to reveal expression of both genes in the same preparation (Fig. 6), shows that there is only slight overlap between the two expression domains. Rather they meet at the blastoderm margin, just where our fate map analysis revealed a border between the notochord domain and cells that express head mesodermal fates (Fig. 3D).

### Mutations of *flh* and *ntl* differentially affect the fates of cells within the notochord domain

The above studies suggest that cells in the notochord domain are distinguished from the cells in all neighboring domains by their expression of *flh*. Hence, *flh* expression at this early stage might serve to define the notochord domain, causing cells within it to adopt the notochord fate, perhaps along with other genes such as *pintallavis* (O'Reilly et al., 1995) or *chordin* (Sasai et al., 1994). In *flh* mutants, expression of a muscle-specific gene, *MyoD* (Weinberg et al., 1996), invades the late gastrula midline (Halpern et al., 1995), and eventually muscle

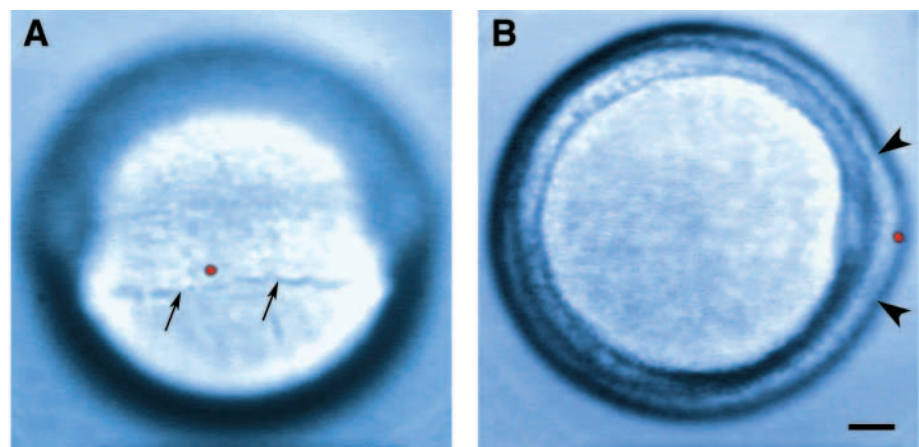


**Fig. 1.** Dorsal (A) and animal pole (B) views of a shield stage embryo with a single labeled cell. Arrows in A indicate the margin of the blastoderm. Arrowheads in B mark the approximate edges of the embryonic shield. Scale bar, 100  $\mu$ m.

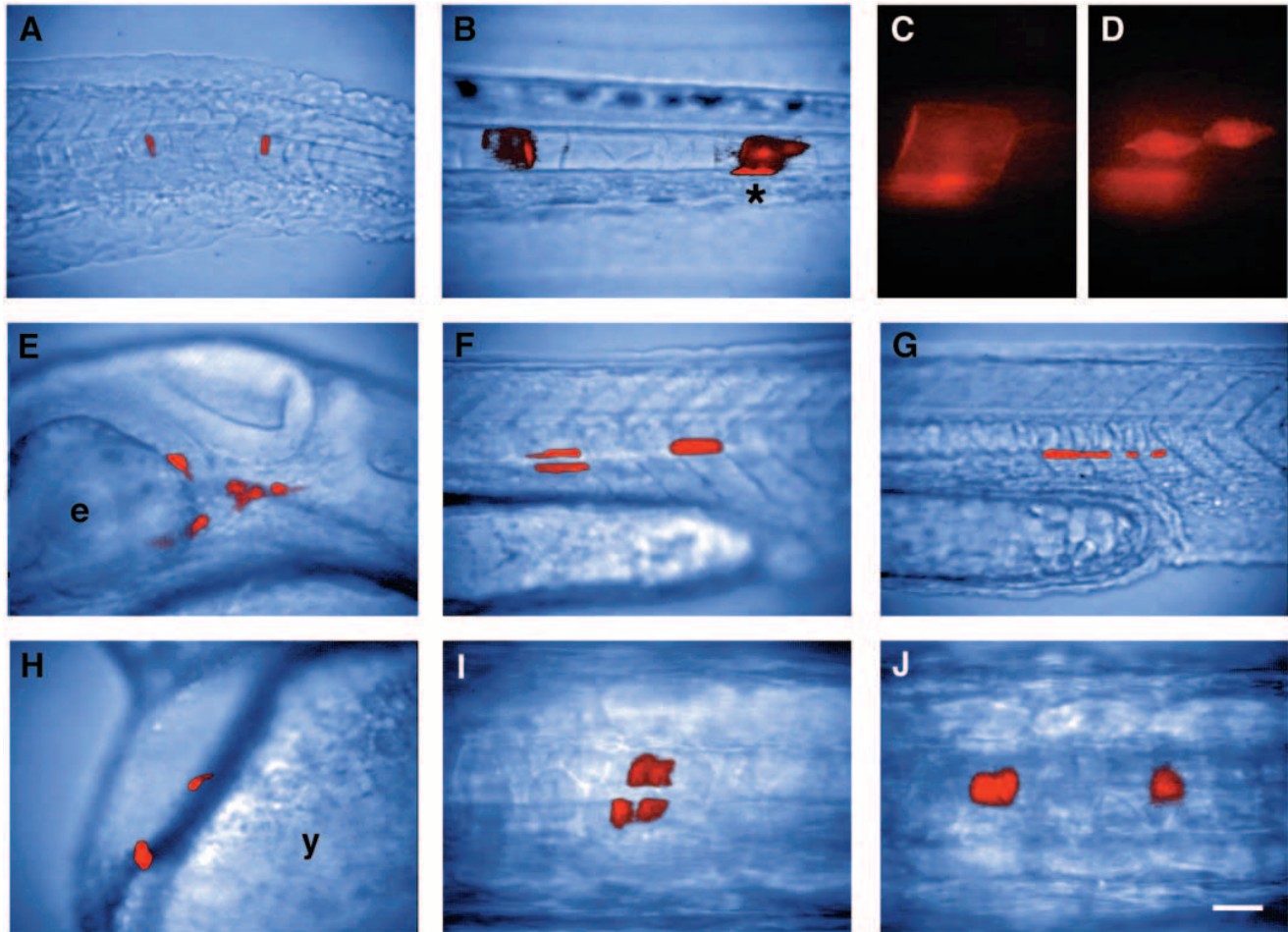


**Fig. 2.** The fates of cells from the dorsal marginal region of the gastrula. (A,E-H) Side views during the early pharyngula period (24-36h); (B-D) side views at 3d; (I,J) dorsal views during the pharyngula period. Anterior is to the left in all panels. A-D show the same embryo, in which coin-shaped cells of the notochord rudiment gave rise to both vacuolated notochord cells and notochord sheath by 2d. (A) The clone initially contained three cells at 1d: one cell anteriorly and two posteriorly. (B) At 3d, the anterior cell had become a vacuolated cell, and the posterior cells had generated one vacuolated cell and four notochord sheath cells. (C,D) Higher power fluorescent views of the posterior cells (asterisk in B) at different focal planes at 3d. (C) Vacuolated cell. (D) Sheath cells. Only two of the four notochord sheath cells are in focus. (E) Head mesenchyme: cells that were ventral and lateral to the brain, and were mesenchymal during the early pharyngula period. We sometimes observed these clones differentiating as endothelial cells ( $n=6$ ) or parachordal cartilage ( $n=2$ ). Head muscles also arise from cells that are mesenchymal at 1d (Schilling and Kimmel, 1994; Kimmel et al., 1990; Warga, 1996). (F) Somitic muscle: these cells spanned the length of the somite. Muscle clones were confined to one side of the animal if located in the trunk, but were often bilateral if located in the tail (Kimmel and Warga, 1987). (G) Hypochochord: an axial tissue lying just below the notochord, and extending from the level of the first somite through the tail. Like the floor plate of the spinal cord, hypochochord is composed of a single midline row of cells in zebrafish (Hatta and Kimmel, 1993). (H) Hatching gland: large granule-filled cells that lie on the surface of the pericardium. (I) Ventral nervous system: these clones included both morphologically identifiable neurons and other cells presumed to be glia or neuroblasts. This clone excluded floor plate. Neuroepithelial cells such as these and floor plate cells have a similar cuboidal morphology in side views, but floor plate can be distinguished in a dorsal view as forming a single midline row of cells. (J) Floor plate: part of a clone derived from a deep cell in the third layer of the epiblast. A,B,E-J are composites of bright-field and fluorescent images taken at the same focal plane; C and D are fluorescent images only. Scale bar, 40  $\mu\text{m}$  in A,B,E-H; 100  $\mu\text{m}$  in C,D,I,J.

differentiates in the mutant midline (Talbot et al., 1995). A possible explanation for these findings is that in the absence of *flh* function, notochord domain cells adopt the muscle fate. We used the fate map to examine this possibility.

When cells within the notochord domain, as defined in wild-type embryos, were labeled in *flh* mutants, they developed as clones of muscle cells (Fig. 7A-E,G). Thus, loss of *flh* function appears to switch the development of cells that normally form notochord to muscle. The phenotypic change to muscle is specific to *flh* mutants. When we labeled notochord domain

cells in *ntl* mutants, they gave rise to axial cells deep to the spinal cord that resembled neither notochord nor muscle, but appeared mesenchymal (Fig. 7F;  $n=9$ ), consistent with a previous study (Halpern et al., 1993).

Interestingly, labeled muscle cells in *flh* mutants were not confined to the midline, but were often located at the lateral edge of the myotomes when observed during the early pharyngula period (Fig. 7C,E). The lateral location of these cells suggests that notochord domain cells in *flh* mutants develop as a subset of the somite, termed adaxial cells. When adaxial cells

develop initially in wild-type embryos, they flank the notochord as the most medial presomitic cells (Thisse et al., 1993; Hammerschmidt and Nüsslein-Volhard, 1993). As shown recently (Devoto et al., personal communication), these cells migrate laterally through the somite to form a distinctive superficial layer of the body wall muscle. In *flh* mutants, some of the labeled muscle cells derived from the gastrula midline domain had medial extensions, and in several cases, processes from individual cells spanned the midline (Fig. 7G). In about half of the clones, muscle cells formed bilaterally (Fig. 7C), which is never observed in clones of muscle in the wild-type trunk (our findings; and Kimmel and Warga, 1987). The bilateral distribution of notochord domain-derived muscle in

*flh* mutants may reflect the lack of any axial boundary in the medially fused myotomes.

### Cells from the region of the notochord domain may join the forerunners and develop tail mesodermal fates

If expression of the *flh* gene normally specifies early gastrula cells at the dorsal blastoderm margin to adopt the notochord fate, then why do some cells present in the notochord domain of wild-type embryos adopt other fates? As described above, we observed a significant change between the fates of notochord domain cells according to whether they developed in the trunk or tail. A subset developed unrestricted fates in the tail, contributing substantially to tail muscle (Fig. 4B) and tail fin mesenchyme (Fig. 4C), and always located in the caudal-most tail segments (caudal to segment 24). Moreover, in each of these features, the subset of unrestricted notochord domain cells resembled the forerunners, cells present in a cluster just beyond the blastoderm margin (Fig. 8A). Since unrestricted notochord-domain cells of the early gastrula eventually expressed the same fates in the same locations as the forerunner cells, it seemed possible that these cells actually leave the blastoderm and join the forerunner population.

To learn if blastoderm cells can indeed become forerunner cells, we labeled cells at the dorsal blastoderm margin at blastula stages, before the forerunners appear. We observed that 2.5-3 hours later, at early gastrula stages, clones descended from the injected marginal cell had contributed progeny to both the hypoblast and the forerunner population (Fig. 8B;  $n=8$ ). The clone illustrated eventually formed mesodermal derivatives in the head (Fig. 8C), and caudal tail mesoderm, including tail muscle and fin mesenchyme (Fig. 8D,E). These are the fates expected to derive, respectively, from the anterior hypoblast (Warga, 1996) and the forerunners (Fig. 4). Hence, at least some of the forerunners arise from the dorsal marginal blastoderm, the region that also forms the notochord domain.

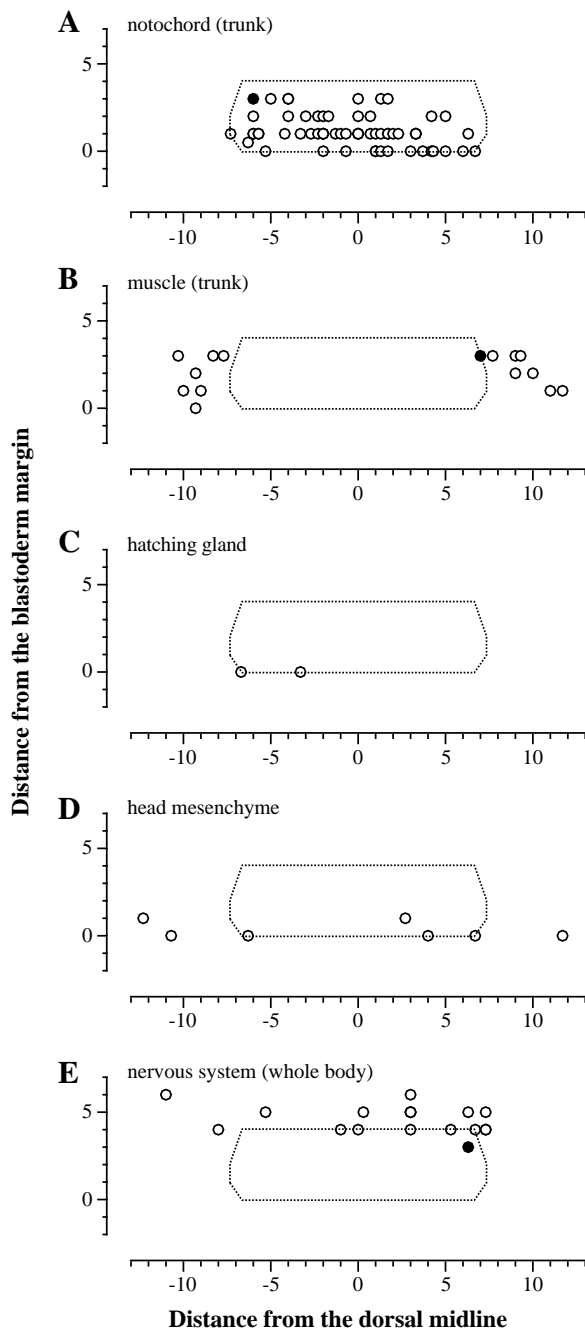


**Fig. 3.** Fate map of the shield region of the gastrula: notochord and muscle in the trunk, anterior mesoderm (hatching gland and head mesenchyme), and nervous system along the length of the body. Derivatives are graphed separately for clarity: (A) notochord, (B) somitic muscle, (C) hatching gland, (D) head mesenchyme, and (E) nervous system. The x- and y-axes are distances, in cell diameters, from the dorsal midline and the blastoderm margin, respectively. The margin of the blastoderm is at zero on the y-axis. Cells are plotted left and right on the map as they were located in the embryo, although we assume that the gastrula is bilaterally symmetrical. The oval shaped outline denotes the outline of the notochord domain, which surrounds the central region containing most of the notochord precursors that we labeled, and is shown on each graph for reference. Open circles represent tissue-restricted cells. Filled circles represent cells that were unrestricted, i.e. their progeny contributed to two or more different tissues. Three cells (out of 162 total cells) gave rise to unrestricted clones for these tissues: one gave rise to trunk muscle and tail notochord; one gave rise to trunk notochord and tail hypochord; and one gave rise to nervous system (including floor plate) and fin mesenchyme in the tail. Some positions in the fate map were labeled multiple times and these appear as only one spot on the graphs; see Table 1 for total numbers of cells labeled.

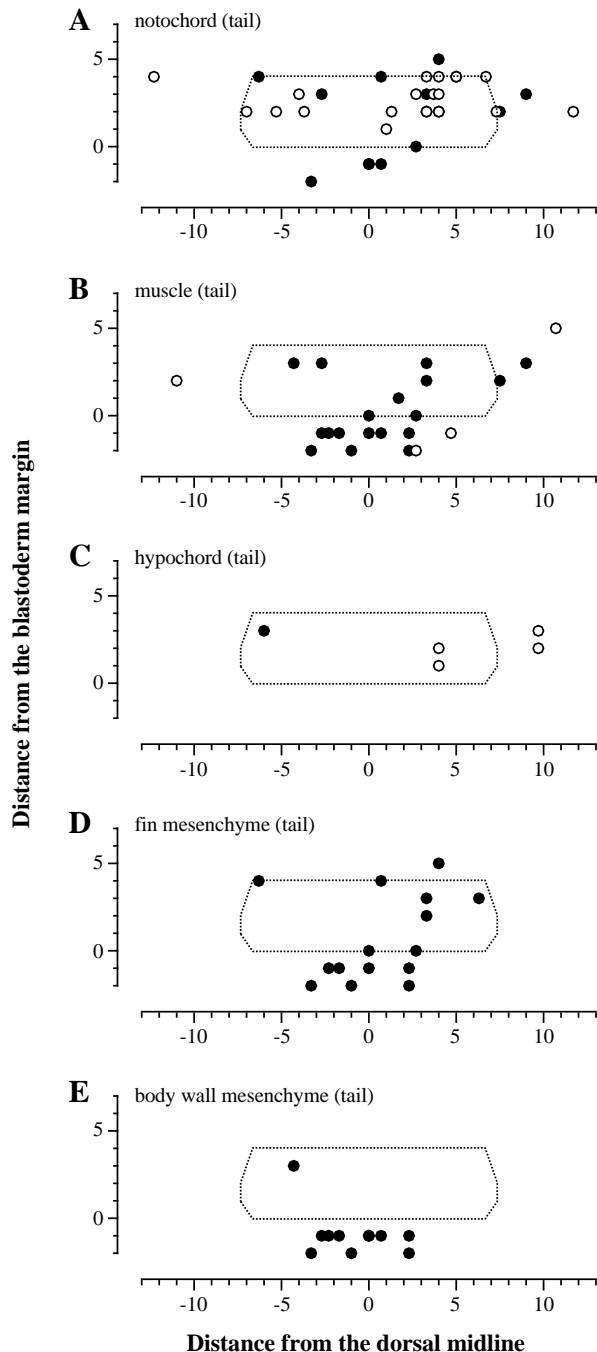


**Fig. 4.** Fate map of the shield region of the gastrula: tail mesoderm. The axes and symbols are the same as in Fig. 3. (A) Notochord, (B) muscle, (C) hypochord. Although the hypochord extends up through the trunk (Hatta and Kimmel, 1993), we only labeled cells that gave rise to hypochord in the tail. (D) Fin mesenchyme. These were mesenchymal cells which migrated into the caudal fin at 2d. Some of these cells had the stellate appearance described for fin mesenchymal cells that migrate along the actinotrichia (Wood and Thorogood, 1984). (E) Body wall mesenchyme. These were cells that were mesenchymal, did not have the appearance of somitic muscle or notochord cells, yet were not located in the fins. Since precursors of tail mesoderm that were unrestricted gave rise to cells in two or more tissues, the same cell appears on different graphs, according to which tissues it contributed progeny. The forerunner cell population corresponds to the negative values on the y-axis (i.e. -1 and -2 denote the first and second rows below the dorsal blastoderm margin).

### Forerunner cells may constitute a specified gastrula domain

The above analysis is consistent with a view that cells joining the forerunners become specified towards the development of a set of tail mesodermal fates, in much the same way that we have supposed that cells in the blastoderm are specified to develop single fates such as the notochord. We watched how the forerunner cells developed during gastrulation and segmentation to learn if they, as a population, exhibited distinctive features that might characterize a specified domain.

We followed forerunner cells labeled singly ( $n=26$ ; data not shown), or labeled collectively with caged fluorescein to reveal the whole population ( $n=12$ ; Fig. 9A,C). Unlike blastoderm cells which involute and then move within the hypoblast towards the animal pole (Warga and Kimmel, 1990), the forerunner cells remain separate from the blastoderm during epiboly, advancing along the yolk syncytial layer ahead of the blastoderm margin. At the end of epiboly, dorsal cells move over the cluster of forerunner cells (Fig. 9A, arrow), bringing the cluster to a deep position within the developing tail bud. Based on its morphology and the comparative expression patterns of *Xnot* and *flh* in this region (Gont et al., 1993; Melby et al., unpublished data), we term this dorsal mass of tissue the chordoneural hinge, described originally by Pasteels (1943). Shortly afterwards, the cluster of forerunner cells swells and forms the cuboidal epithelium of Kupffer's vesicle (Fig. 9C), a fluid-filled sac that has been known for many years as an enigmatic specialty of the developing teleost tail (reviewed by Nordahl, 1970). Our evidence suggests that all, or nearly all, of the cells of Kupffer's vesicle derive from the forerunner population. Using different dye-labeling techniques and confocal time-lapse microscopy, Cooper and D'Amico (personal communication) have made similar observations about the development and fate of the forerunner cells. Near the end of the segmentation period Kupffer's vesicle disappears. The forerunner cell descendants that had transiently formed its lining later develop mesodermal fates near the end of the tail (Fig. 8D,E).

### Forerunner cells fail to form Kupffer's vesicle in *ntl* mutants

Since the forerunner cells are prominently involved in tail development it was of interest to examine them in *ntl* mutants, in which tail development aborts (Halpern et al., 1993). We observed that forerunner cells are present in the early gastrula in *ntl* mutants, and we did not find systematic changes in their numbers or pattern of movements during epiboly (data not shown). However, *ntl* mutants never develop Kupffer's vesicle (Fig. 10B), in contrast to wild-type embryos in which we could see it in 97% of embryos, and in contrast to *flh* mutants, in which we could identify the vesicle in 75% of embryos (Fig. 10A,C; Table 2). We followed the development of forerunner cells labeled by uncaging, and observed that the first apparent change in *ntl* mutants occurs just after epiboly. At this time the forerunner cluster is present adjacent to, rather than deep to the chordoneural hinge as in wild types (compare Fig. 9A and B). The forerunner cells then remain densely clustered in *ntl* mutants (Fig. 9D) during the stages that Kupffer's vesicle forms in the wild type.

The inability of the forerunner cells to differentiate a

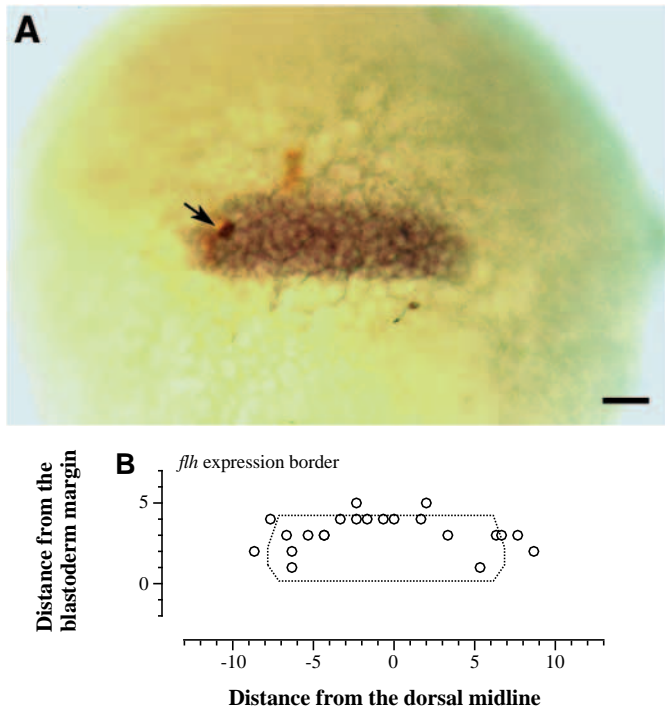


**Fig. 5.** The *flh* RNA expression domain coincides with the notochord domain at the early gastrula stage. (A) Dorsal view of a double labeled gastrula. The cell marked with lineage tracer is stained brown (black arrow) and *flh* RNA is greenish-brown. Scale bar: 50  $\mu$ m. (B) Map of the border of strongest *flh* expression. The axes of the graph are as in Fig. 3. Open circles represent the border of strongest *flh* expression determined relative to the coordinates of labeled cells. In some cases, both a lateral and a posterior boundary point were determined from a single labeled cell. The border of *flh* expression is defined as the outermost cell strongly expressing *flh* RNA.

Kupffer's vesicle in *ntl* mutants might be a cell-autonomous effect of the mutation, since the *ntl* gene is normally expressed in the forerunners (Hammerschmidt and Nusslein-Volhard, 1993; Melby et al., 1993; Schulte-Merker et al., 1994b). We observe that *ntl* RNA expression persists in this population in both wild type and *ntl* mutants during the early segmentation stages when the vesicle normally forms (Fig. 10E,F). Labeling of the cluster is especially clear during this period in *ntl* mutants, because unlike wild-type embryos, there is no *ntl* RNA expression in the axial notochord domain to obscure the labeling of the forerunner cluster. In *ntl* mutants, expression of the defective RNA persists in the cluster through the early segmentation period (see also Schulte-Merker et al., 1994b). By the time that Kupffer's vesicle is well-formed in wild-type embryos (e.g. 7-somite stage), *ntl* expression in mutants is lost in the cluster (data not shown).

## DISCUSSION

### Specification to a notochord-forming cellular domain

We have fate mapped a domain of cells that mostly generate notochord, with the exception of a minority of cells in the domain that contribute to the caudal-most tail, which we will

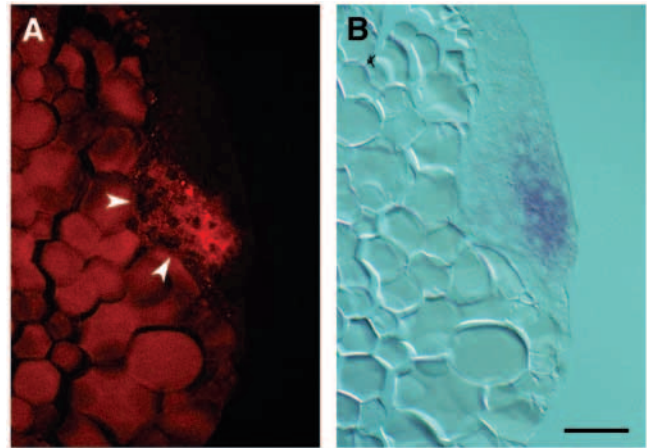


**Fig. 6.** *flh* expression in the early gastrula does not substantially overlap with *gsc* expression. (A) Epifluorescent (Texas Red filter set) and (B) bright-field views of a mid-sagittal section through the embryonic shield of an early gastrula that was hybridized with probes for both *gsc* (red) and *flh* (blue) RNA. White arrowheads in A indicate red fluorescence due to *gsc* expression in involuted cells (the yolk is autofluorescent at this wavelength). B shows *flh* expression is restricted to the epiblast. Scale bar, 50  $\mu$ m.

consider below. The cells are in the superficial layer of the epiblast in the embryonic shield, shortly after the beginning of involution in the early gastrula. We did not extend the mapping to deeper cells, some of which also generate notochord (Shih and Fraser, 1995). The boundaries are sharp; the notochord domain does not overlap with adjacent fate map domains. The boundaries coincide at a cellular level of resolution with the expression boundaries of *flh*, a gene that we show when mutated causes cells of the notochord domain to change to a muscle fate. Based on our observations, and on results reported elsewhere (Talbot et al., 1995; Halpern et al., 1995) we postulate that *flh* is a key component of a genetic network that acts in the early gastrula to specify cells to adopt the notochord fate.

Most early gastrula cells, even when located at a fate map domain boundary, produce clones that are tissue-restricted: all of the clonally related cells develop the same tissue or organ fate. Restriction might mean that the clonal descendants cell-autonomously inherit the specified states of their early gastrula progenitors. However, this explanation seems unlikely, because heterotopically transplanted early gastrula cells develop fates in accordance with their new surroundings (Ho and Kimmel, 1993). Moreover, transplanted cells can reversibly switch gene expression, as assayed by *ntl* gene expression (Schulte-Merker et al., 1992), which might in part account for their plasticity in cell fate decisions. Hence, although notochord domain cells were not studied specifically in these transplantation experiments, it seems likely that notochord domain cells are uncommitted at the early gastrula stage when they specifically express *flh*, and generate notochord-restricted clones. It may be that early gene expression somehow biases the cells in a fate map domain to develop together as a cohort, which would account for clonal restriction, and 'conditional' specification (Davidson, 1990, 1993). According to this view, remaining within the notochord domain and continuing expression of the *flh* gene are both essential for cells to maintain notochord identity.

The topological position and relation to adjacent fate map regions that we describe for the notochord domain are similar to those described for other vertebrates, including frog (Keller, 1975; 1976), chick (Selleck and Stern, 1991; Schoenwolf et al., 1992; Garcia-Martinez et al., 1993) and mouse (Lawson et al., 1991; Smith et al., 1994). Our data are consistent with a previous fate map made in zebrafish from injections into blastula cells (Kimmel et al., 1990), and with the morphogenetic movements of dorsal convergence and involution at the margin that have been described for zebrafish gastrulation (Warga and Kimmel, 1990). Our findings do not confirm the report (Shih and Fraser, 1995) that cells generating neural, somitic, and endodermal fates are intermingled with notochord progenitors in the zebrafish early gastrula embryonic shield, including the superficial epiblast cells we examined. In particular, we do not find neural progenitors, including floor plate progenitors, to be very close to the blastoderm margin.

#### Loss of *flh* function respecifies cells of the notochord domain

We suggest (see also Halpern et al., 1995) that expression of the wild-type *flh* gene must be maintained in notochord domain cells, at least through gastrulation, for them to develop as notochord. The proposal is based in part from our fate map studies showing that notochord domain cells make muscle in *flh* mutants, and in part on gene expression studies in *flh* mutants. In particular, expression of the notochord marker *twist* (Halpern et al., 1995), and of the mutant *flh* mRNA (Melby et al., unpublished data) appears essentially the same as in wild-type embryos during early gastrulation. After midgastrulation, a time when cells begin to become committed to tissue fates (Ho and Kimmel, 1993), midline involuted cells in *flh* mutant embryos lose *flh* RNA expression (Melby et al., unpublished data) and take on a paraxial character, now expressing *MyoD* and *snail1* (Halpern et al., 1995). Hence, *flh* function is not essential to set up the notochord domain in the early gastrula, but is ultimately required for the notochord to develop. Understanding *flh* to function not as a 'master' regulatory gene, but as a component of a gene network (Weintraub, 1993) that might include *ntl*, *twist*, and *chordin* (Sasai et al.,

1994) among others, may explain why the early expression domains appear normal in *flh* mutants.

#### Notochord-domain cells generating tail fates may be respecified

We postulate that for cells to give rise to notochord, they must remain within the notochord domain as they develop, at least

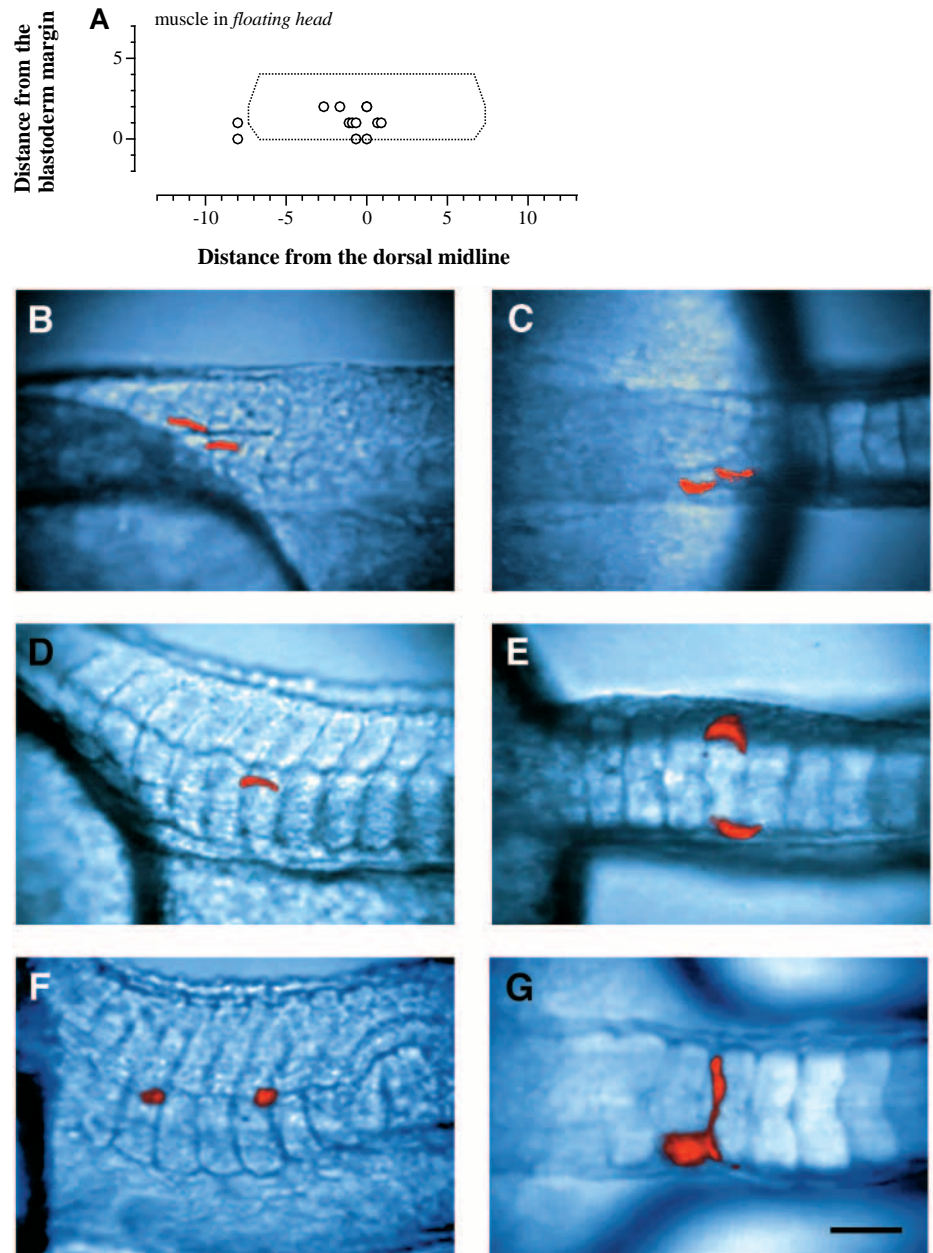


**Fig. 7.** The fate of cells from the notochord domain in *flh* and *ntl* mutant embryos. (A) Map of the cells labeled in *flh* mutant embryos which gave rise to muscle. 10 of these cells fall within the boundary of the notochord domain. In wild-type embryos, 61 of 71 cells labeled within this boundary gave rise to notochord exclusively. The axes of the graph are as in Fig. 3. (B-E,G) *flh* and (F) *ntl* mutant embryos during the early pharyngula period, containing clones of cells derived from single labeled cells in the notochord domain of the gastrula. Side (B) and dorsal (C) views of a unilateral clone of muscle cells in a *flh* embryo. Side (D) and dorsal (E) views of a bilateral muscle clone in a *flh* embryo. (F) Side view of a clone of axial mesenchymal cells derived from a notochord domain cell in a *ntl* embryo. (G) Dorsal view of a clone containing a cell that spanned the midline in a *flh* embryo. Scale bar, 50  $\mu$ m.

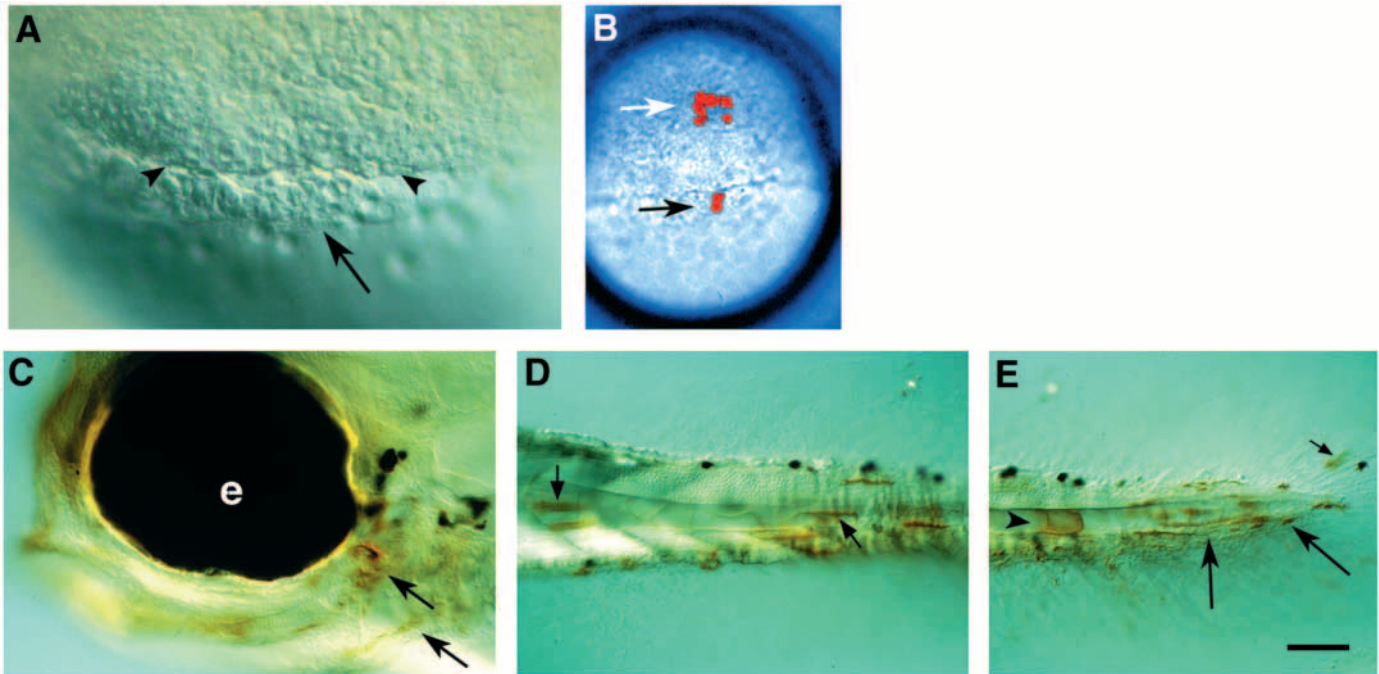
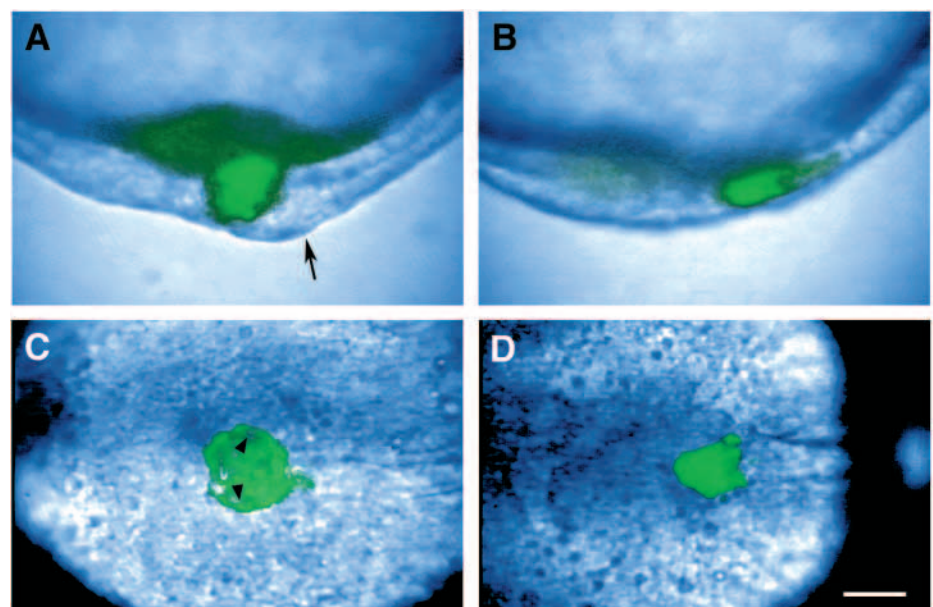


**Fig. 8.** Dorsal marginal blastomeres can contribute to the forerunner cells. (A) Nomarski optics photograph showing the appearance of the forerunner cells at shield stage. Arrow points to the forerunner cell cluster, and arrowheads point to the margin of the blastoderm. B-E are from an embryo in which a labeled marginal blastomere contributed to both anterior mesoderm and forerunner cell derivatives. (B) Dorsal view of the live embryo at late shield stage. The clone consists of a cluster of cells in the anterior hypoblast (white arrow) and two cells in the forerunner cell population (black arrow). (C-E) Whole-mount side views of the embryo at 3d, after it had been fixed and stained for the lineage label, biotin. Biotin staining appears brown, while pigment cells appear black. (C) The head region, showing labeled pharyngeal endoderm (arrows), derived from cell(s) in the anterior hypoblast. e, eye. (D) Part of the tail showing labeled muscle cells (arrows). (E) More posterior view of the tail showing labeled notochord (arrowhead), body wall mesenchyme (arrows), and fin mesenchyme (small arrow). Scale bar: 40  $\mu\text{m}$  in A; 250  $\mu\text{m}$  in B; 50  $\mu\text{m}$  in C-E.

through most of gastrulation. This postulate provides an explanation for our observation that fates other than notochord can arise from cells located in the early gastrula notochord domain. These cells generate a characteristic set of mesodermal fates

similar to forerunner clones, including notochord, muscle, and fin mesenchyme in the caudal-most tail segments. We suppose, in this case, that cells leave the notochord domain, perhaps just as they undergo involution at the blastoderm margin, and join

**Fig. 9.** Caged fluorescein labeling of the forerunner population in wild-type and *ntl* mutant embryos. Composite video images of caged fluorescein labeling in wild-type (A,C) and *ntl* mutant (B,D) embryos. The forerunner cell population was labeled by uncaging during the early gastrula period (5.5-6.5h). Fluorescein-labeled cells are colored green. (A,B) Side views of the tailbud at the bud stage. Dorsal is to the right. In wild-type embryos, there is labeling in a cluster of cells located deep to the chordoneural hinge (arrow), the larger tissue mass on the dorsoanterior side of the tailbud. In *ntl* mutant embryos at the bud stage, the forerunner cell cluster appears to be adjacent to the chordoneural hinge, and the ventral side of the tailbud is proportionately larger. (C,D) Dorsal views of the tailbud at the 7-somite stage. The axial mesoderm extends anteriorly to the right. (C) By this stage, Kupffer's vesicle is obvious in the tailbud of wild-type embryos, arrowheads point to the inside wall of the vesicle. Cells lining Kupffer's vesicle are specifically labeled. (D) In contrast, fluorescein-labeled cells in *ntl* mutant embryos remain in a tight cluster. Scale bar, 50  $\mu\text{m}$  in A,B; 72  $\mu\text{m}$  in C,D.



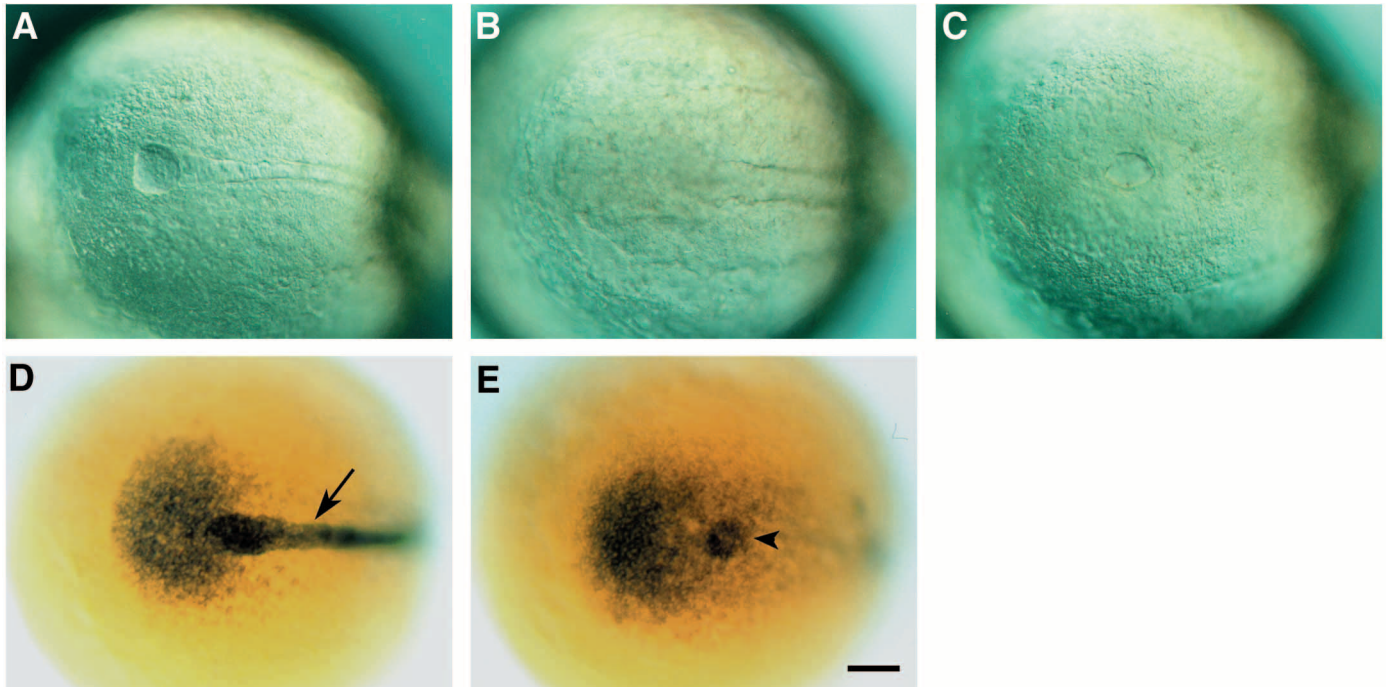


**Fig. 10.** The *ntl* gene is required for the formation of Kupffer's vesicle. (A-C) Kupffer's vesicle never forms in *ntl* mutants, but can form in *flh* mutants. Nomarski optics photographs of dorsal views of the tailbuds of live wild-type (A), *ntl* (B), and *flh* (C) mutant embryos. Anterior extends to the right. (A) In wild-type embryos, Kupffer's vesicle is large and prominent, lying below the end of the forming notochord. (B) In *ntl* mutant embryos, no vesicle forms, however boundaries between axial and paraxial mesoderm can be seen. (C) In *flh* mutant embryos, Kupffer's vesicle often forms, but it is smaller and less regularly shaped than in wild-type embryos. Axial-paraxial boundaries are absent. (D,E) Expression of *ntl* RNA as a marker for forerunner cell development in wild-type (D) and *ntl* mutant (E) embryos. Dorsal views of the tailbud at the 2-3-somite stage; anterior extends to the right. (D) In wild-type embryos, *ntl* RNA is expressed in cells located posteriorly in the tailbud, and in the cells of the forming notochord (arrow). *ntl* RNA is also expressed by cells of the forerunner cluster that will form Kupffer's vesicle, but this labeling is obscured by labeling in the overlying notochord rudiment. (E) In *ntl* mutant embryos, there is an absence of labeling in the axial mesoderm, so labeling in the forerunner cluster is obvious (arrowhead). Scale bar: 50  $\mu$ m.

the forerunners. This particular model would explain why cells can express forerunner fates irrespective of their distance from the blastoderm margin: cells at different distances would all pass by the forerunners as they involute (albeit at different times).

Our data do not directly show cells leaving the notochord domain and joining the forerunner domain. To do so would require observing large numbers of labeled clones as they developed through gastrulation, since only a minority of cells in the notochord domain (11 out of 91; 12%) generate tail mesodermal fates and would thus exhibit domain-switching behavior. However, as indirect support of our argument, we did verify that blastoderm cells, labeled at earlier times and present in the region from which the notochord domain arises, can leave the blastoderm and join the forerunners.

An alternative to our specific proposal that notochord domain cells join the forerunners during gastrulation is that the domain-switching might occur later in the developing tail bud. This switch would occur after midgastrulation, when we suppose cellular commitments arise (Ho and Kimmel, 1993), at least for anterior fates; however, no one has studied commitments to tail fates, which could well occur substantially later. The issue requires time-lapse study of labeled notochord domain clones through gastrulation and perhaps early segmentation periods, which would permit correlation of the morphogenetic behaviors of individual developing cells with the fates they later express.

### The role of the forerunner cells in tail development

The forerunners appear to be a specified fate map domain in the gastrula. Although they generate unrestricted mesoderm in the pharyngula, they are specifically fated to form Kupffer's vesicle during the segmentation period, and in addition show segregation from the blastoderm and unique morphogenesis during gastrulation. It should be made clear that the forerunner cells do not constitute a 'tail-forming region' as has been mapped in the *Xenopus* neurula (Tucker and Slack, 1995), since they contribute only a subset of the total mesoderm cells in the caudal-most segments (Melby, unpublished observations). We hypothesize that once forerunners have fulfilled their function in forming Kupffer's vesicle, which is present only transiently, that they then rejoin tail morphogenesis, perhaps becoming dispersed among domains that will generate the caudal-most tail mesoderm.

Our observation that Kupffer's vesicle never forms in *ntl* mutants suggests that the vesicle might have some role in the organization of tail development. However, the failure to differentiate Kupffer's vesicle might not be a cause, but just a consequence of disrupted tail development. Studies of the homologous mouse mutation *Brachyury* have indicated that this gene might be involved in controlling cell movements: mutant cells may have altered adhesive properties which disrupt posterior morphogenesis (Hashimoto et al., 1987; Wilson et al., 1993, 1995). We find that in *ntl* mutants, *flh* RNA

shows a broad and diffuse triangular-shaped domain of expression in the tailbud, compared to the narrow axial stripe of expression seen in wild type (Melby et al., unpublished data). The alteration in the *flh* expression pattern could be interpreted as resulting from a failure of mutant tailbud cells to converge to the midline. Hence, the lack of Kupffer's vesicle in *ntl* mutants might result from the disruption of an interaction between forerunner cells and the overlying axial mesoderm. Alternatively, Kupffer's vesicle itself might form some sort of signaling center which directs the morphogenesis of tailbud cells. Determining whether Kupffer's vesicle has an instructive role during zebrafish tail organization will require mosaic analysis, and a thorough investigation of tail morphogenesis.

## Conclusion

Based on the organization of the fate map and the correlation of *flh* expression with notochord fate restriction, we propose that the early gastrula contains a specified notochord domain. Similarly, a variety of other genes (*eve1*, Joly et al., 1993; *gsc*, Stachel et al., 1993; Thisse et al., 1994; *ntl*, Schulte-Merker et al., 1992, 1994a,b; *axial*, Strahle et al., 1993; *zffh1*, Warga et al., unpublished data) have been described that are expressed in subsets of cells during the early gastrula stage. We suspect that these patterns of gene expression indicate that many cells in the early gastrula have begun to be channeled along distinct developmental pathways, and that the notochord domain that we have identified will be just one of many specified domains in the early gastrula.

We thank M. S. Cooper and L. D'Amico for sharing results prior to publication. We also gratefully acknowledge D. W. Raible, M. E. Halpern, D. Kimelman, W. S. Talbot and particularly J. S. Eisen for critical reading of the manuscript. The work was supported by NIH grants HD22486. A. E. M. was supported by NIH predoctoral training grants GM07257 and HD07348.

## REFERENCES

- Davidson, E. H. (1990). How embryos work: a comparative view of diverse modes of cell fate specification. *Development* **108**, 365-389.
- Davidson, E. H. (1993). Later embryogenesis: regulatory circuitry in morphogenetic fields. *Development* **118**, 665-690.
- Fan, C. M. and Tessier Lavigne, M. (1994). Patterning of mammalian somites by surface ectoderm and notochord: evidence for sclerotome induction by a *hedgehog* homolog. *Cell* **79**, 1175-1186.
- Garcia Martinez, V., Alvarez, I. S. and Schoenwolf, G. C. (1993). Locations of the ectodermal and nonectodermal subdivisions of the epiblast at stages 3 and 4 of avian gastrulation and neurulation. *J. Exp. Zool.* **267**, 431-446.
- Gont, L. K., Steinbeisser, H., Blumberg, B. and De Robertis, E. M. (1993). Tail formation as a continuation of gastrulation: the multiple cell populations of the *Xenopus* tailbud derive from the late blastopore lip. *Development* **119**, 991-1004.
- Halpern, M. E., Ho, R. K., Walker, C. and Kimmel, C. B. (1993). Induction of muscle pioneers and floor plate is distinguished by the zebrafish *no tail* mutation. *Cell* **75**, 99-111.
- Halpern, M. E., Thisse, C., Ho, R. K., Thisse, B., Riggelman, B., Trevarrow, B., Weinberg, E. S., Postlethwait, J. H. and Kimmel, C. B. (1995). Cell-autonomous shift from axial to paraxial mesodermal development in zebrafish *floating head* mutants. *Development* **121**, 4257-4264.
- Hammerschmidt, M. and Nüsslein-Volhard, C. (1993). The expression of a zebrafish gene homologous to *Drosophila snail* suggests a conserved function in invertebrate and vertebrate gastrulation. *Development* **119**, 1107-1118.
- Hashimoto, K., Fujimoto, H. and Nakatsuji, N. (1987). An ECM substratum allows mouse mesodermal cells isolated from the primitive streak to exhibit motility similar to that inside the mouse embryo and reveals a deficiency in the *T/T* mutant cells. *Development* **100**, 587-598.
- Hatta, K. and Kimmel, C. B. (1993). Midline structures and central nervous system coordinates in zebrafish. *Perspect. Dev. Neurobiol.* **1**, 257-268.
- Hatta, K., Kimmel, C. B., Ho, R. K. and Walker, C. (1991). The *cyclops* mutation blocks specification of the floor plate of the zebrafish central nervous system. *Nature* **350**, 339-341.
- Hauptmann, G. and Gerster, T. (1994). Two-color whole-mount in situ hybridization to vertebrate and *Drosophila* embryos. *Trends Genet.* **10**, 266.
- Ho, R. K. (1992). Axis formation in the embryo of the zebrafish, *Brachydanio rerio*. *Sem. Dev. Biol.* **3**, 53-64.
- Ho, R. K. and Kane, D. A. (1990). Cell-autonomous action of zebrafish *spt-1* mutation in specific mesodermal precursors. *Nature* **348**, 728-730.
- Ho, R. K. and Kimmel, C. B. (1993). Commitment of cell fate in the early zebrafish embryo. *Science* **261**, 109-111.
- Joly, J. S., Joly, C., Schulte-Merker, S., Boulekbache, H. and Condamine, H. (1993). The ventral and posterior expression of the zebrafish homeobox gene *eve1* is perturbed in dorsalized and mutant embryos. *Development* **119**, 1261-1275.
- Jowett, T. and Lettice, L. (1994). Whole-mount in situ hybridizations on zebrafish embryos using a mixture of digoxigenin- and fluorescein-labeled probes. *Trends Genet.* **10**, 73-74.
- Keller, R. E. (1975). Vital dye mapping of the gastrula and neurula of *Xenopus laevis*. I. Prospective areas and morphogenetic movements of the superficial layer. *Dev. Biol.* **42**, 222-241.
- Keller, R. E. (1976). Vital dye mapping of the gastrula and neurula of *Xenopus laevis*. II. Prospective areas and morphogenetic movements of the deep layer. *Dev. Biol.* **51**, 118-137.
- Kimmel, C. B., Ballard, W. W., Kimmel, S. R., Ullmann, B. and Schilling, T. F. (1995). Stages of embryonic development of the zebrafish. *Dev. Dyn.* **203**, 253-310.
- Kimmel, C. B., Kane, D. A. and Ho, R. K. (1991). Lineage specification during early embryonic development of the zebrafish. In *Cell-Cell Interactions in Early Development* (J. Gerhart, Ed.), pp. 203-225. New York: Wiley-Liss, Inc.
- Kimmel, C. B. and Warga, R. M. (1987). Cell lineages generating axial muscle in the zebrafish embryo. *Nature* **327**, 234-237.
- Kimmel, C. B., Warga, R. M. and Schilling, T. F. (1990). Origin and organization of the zebrafish fate map. *Development* **108**, 581-594.
- Kispert, A. and Hermann, B. G. (1993). The *Brachyury* gene encodes a novel DNA binding protein. *EMBO J.* **12**, 4898-4899.
- Koseki, H., Wallin, J., Wilting, J., Mizutani, Y., Kispert, A., Ebensperger, C., Herrmann, B. G., Christ, B. and Balling, R. (1993). A role for *Pax-1* as a mediator of notochordal signals during the dorsoventral specification of vertebrae. *Development* **119**, 649-660.
- Krauss, S., Concordet, J. P. and Ingham, P. W. (1993). A functionally conserved homolog of the *Drosophila* segment polarity gene *hh* is expressed in tissues with polarizing activity in zebrafish embryos. *Cell* **75**, 1431-1444.
- Lawson, K. A., Meneses, J. J. and Pedersen, R. A. (1991). Clonal analysis of epiblast fate during germ layer formation in the mouse embryo. *Development* **113**, 891-911.
- Melby, A. E., Ho, R. K. and Kimmel, C. B. (1993). An identifiable domain of tail-forming cells in the zebrafish gastrula. *Soc. Neurosci. Abs.* **19**, 445.
- Myers, P. Z. and Bastiani, M. J. (1991). NeuroVideo: a program for capturing and processing time-lapse video. *Comput. Methods Programs Biomed.* **34**, 27-33.
- Nordahl, I. R. (1970). The development and morphology of Kupffer's vesicle in the plaice *Pleuronectes platessa* (L.) and in the cod, *Gadus morhua* L. *Sarsia* **42**, 41-62.
- O'Reilly, M. A., Smith, J. C. and Cunliffe, V. (1995). Patterning of the mesoderm in *Xenopus*: dose-dependent and synergistic effects of *Brachyury* and *Pintallavis*. *Development* **121**, 1351-1359.
- Oppenheimer, J. M. (1936). Processes of localization in developing *Fundulus*. *J. Exp. Biol.* **73**, 405-444.
- Pasteels, J. (1943). Proliférations et croissance dans la gastrulation et la formation de la queue des Vertébrés. *Arch. Biol.* **54**, 2-51.
- Raible, D. W., Wood, A., Hodsdon, W., Henion, P. D., Weston, J. A. and Eisen, J. S. (1992). Segregation and early dispersal of neural crest cells in the embryonic zebrafish. *Dev. Dyn.* **195**, 29-42.
- Sasai, Y., Lu, B., Steinbeisser, H., Geissert, D., Gont, L. K. and De Robertis, E. M. (1994). *Xenopus chordin*: a novel dorsalizing factor activated by organizer-specific homeobox genes. *Cell* **79**, 779-790.
- Schilling, T. F. and Kimmel, C. B. (1994). Segment and cell type lineage

- restrictions during pharyngeal arch development in the zebrafish embryo. *Development* **120**, 483-494.
- Schoenwolf, G. C., Garcia Martinez, V. and Dias, M. S.** (1992). Mesoderm movement and fate during avian gastrulation and neurulation. *Dev. Dyn.* **193**, 235-248.
- Schulte Merker, S., Ho, R. K., Herrmann, B. G. and Nüsslein-Volhard, C.** (1992). The protein product of the zebrafish homologue of the mouse *T* gene is expressed in nuclei of the germ ring and the notochord of the early embryo. *Development* **116**, 1021-1032.
- Schulte-Merker, S., Hammerschmidt, M., Beuchle, D., Cho, K. W., De Robertis, E. M. and Nüsslein-Volhard, C.** (1994a). Expression of zebrafish *gooseoid* and *no tail* gene products in wild-type and mutant *no tail* embryos. *Development* **120**, 843-852.
- Schulte-Merker, S., van Eeden, F. J., Halpern, M. E., Kimmel, C. B. and Nusslein-Volhard, C.** (1994b). *no tail (ntl)* is the zebrafish homologue of the mouse *T (Brachyury)* gene. *Development* **120**, 1009-1015.
- Selleck, M. A. and Stern, C. D.** (1991). Fate mapping and cell lineage analysis of Hensen's node in the chick embryo. *Development* **112**, 615-626.
- Shih, J. and Fraser, S. E.** (1995). Distribution of tissue progenitors within the shield region of the zebrafish gastrula. *Development* **121**, 2755-2765.
- Slack, J. M. W.** (1991). *From Egg to Embryo: Regional Specification in Early Development*. Cambridge: Cambridge University Press.
- Smith, J. L., Gesteland, K. M. and Schoenwolf, G. C.** (1994). Prospective fate map of the mouse primitive streak at 7.5 days of gestation. *Dev. Dyn.* **201**, 279-89.
- Spemann, H. and Mangold, H.** (1924). Über Induktion von Embryonalanlagen durch Implantation artfremder Organismen. *Roux' Arch. Dev Biol.* **100**, 599-638.
- Stachel, S. E., Grunwald, D. J. and Myers, P. Z.** (1993). Lithium perturbation and *gooseoid* expression identify a dorsal specification pathway in the pregastrula zebrafish. *Development* **117**, 1261-1274.
- Strähle, U., Blader, P., Henrique, D. and Ingham, P. W.** (1993). *axial*, a zebrafish gene expressed along the developing body axis, shows altered expression in *cyclops* mutant embryos. *Genes Dev.* **7**, 1436-1446.
- Streisinger, G., Singer, F., Walker, C., Knauber, D. and Dower, N.** (1986). Segregation analysis and gene-centromere distances in zebrafish. *Genetics* **112**, 311-319.
- Talbot, W., Trevarrow, W., Halpern, M. E., Melby, A. E., Farr, H., Postlethwait, J. H., Jowett, T., Kimmel, C. B. and Kimelman, D.** (1995). Requirement for the homeobox gene *floating head* in zebrafish notochord development. *Nature* **378**, 150-157.
- Thisse, C., Thisse, B., Halpern, M. E. and Postlethwait, J. H.** (1994). *gooseoid* expression in neurectoderm and mesendoderm is disrupted in zebrafish *cyclops* gastrulas. *Dev. Biol.* **164**, 420-429.
- Thisse, C., Thisse, B., Schilling, T. F. and Postlethwait, J. H.** (1993). Structure of the zebrafish *snail1* gene and its expression in wild-type, *spadetail* and *no tail* mutant embryos. *Development* **119**, 1203-1215.
- Tucker, A. S. and Slack, J. M. W.** (1995). The *Xenopus laevis* tail-forming region. *Development* **121**, 249-262.
- von Dassow, G., Schmidt, J. E. and Kimelman, D.** (1993). Induction of the *Xenopus* organizer: expression and regulation of *Xnot*, a novel FGF and activin-regulated homeo box gene. *Genes Dev.* **7**, 355-66.
- Warga, R. M.** (1996). Origin and specification of the endoderm in the zebrafish. Ph.D. Dissertation, University of Tübingen, Germany.
- Warga, R. M. and Kimmel, C. B.** (1990). Cell movements during epiboly and gastrulation in zebrafish. *Development* **108**, 569-580.
- Weinberg, E. S., Allende, M. L., Kelly, C. S., Abdelhamid, A., Murakami, T., Andermann, P., Doerre, O. G., Grunwald, D. J. and Riggleman, B.** (1996). Developmental regulation of zebrafish *MyoD* in wild-type, *no tail* and *spadetail* embryos. *Development* **122**, 271-280.
- Weintraub, H.** (1993). The *MyoD* family and myogenesis: redundancy, networks, and thresholds. *Cell* **75**, 1241-4.
- Westerfield, M.** (1994). *The Zebrafish Book. A guide for the laboratory use of zebrafish*. Oregon: University of Oregon Press.
- Wilson, V., Manson, L., Skarnes, W. C. and Beddington, R. S.** (1995). The *T* gene is necessary for normal mesodermal morphogenetic cell movements during gastrulation. *Development* **121**, 877-886.
- Wilson, V., Rashbass, P. and Beddington, R. S.** (1993). Chimeric analysis of *T (Brachyury)* gene function. *Development* **117**, 1321-1331.
- Wood, A. and Thorogood, P.** (1984). An analysis of *in vivo* cell migration during teleost fin morphogenesis. *J. Cell Sci.* **66**, 205-222.
- Yamada, T., Placzek, M., Tanaka, H., Dodd, J. and Jessell, T. M.** (1991). Control of cell pattern in the developing nervous system: polarizing activity of the floor plate and notochord. *Cell* **64**, 635-647.